



*Supplement of*

## **Comparative experimental validation of microwave hyperspectral atmospheric soundings in clear-sky conditions**

**Lei Liu et al.**

*Correspondence to:* Lei Liu (lei.liu5@mail.mcgill.ca)

The copyright of individual parts of the supplement might differ from the article licence.

## S1: Retrieval configurations

This section presents the vertical level adopted and main matrices used in this study, including  $S_e$ ,  $S_a$ , and  $K$  at selected levels.

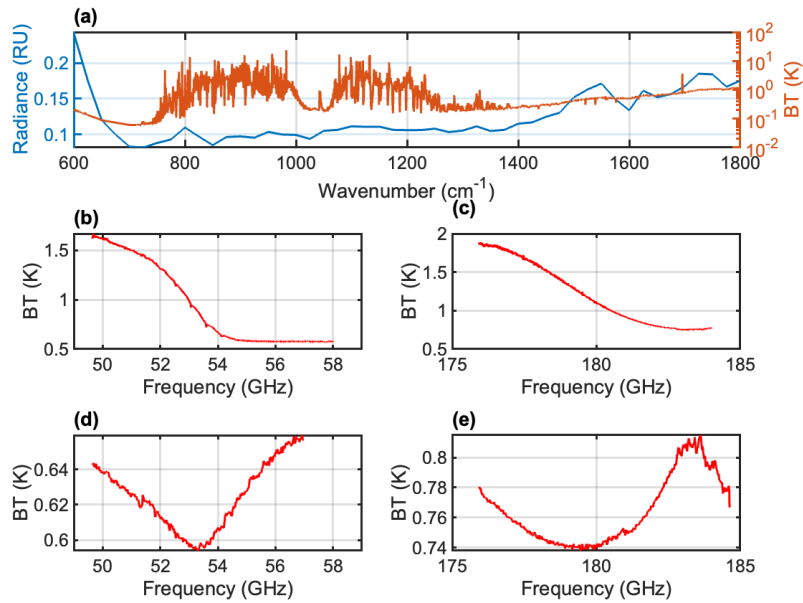


Figure S1. The square root of the diagonal components of  $S_e$  for AERI measurements (a), HiSRAMS nadir-pointing measurements at 6.8 km in the oxygen band (b) and in the water vapor band (c), and HiSRAMS zenith-pointing measurements at the surface in the oxygen band (d) and in the water vapor band (e).

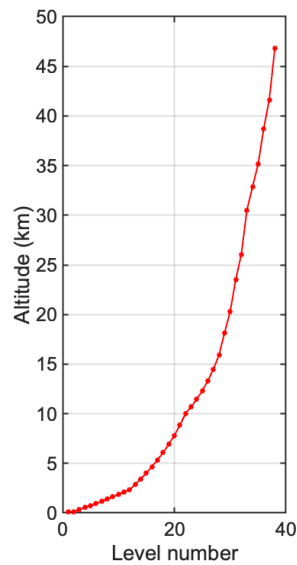
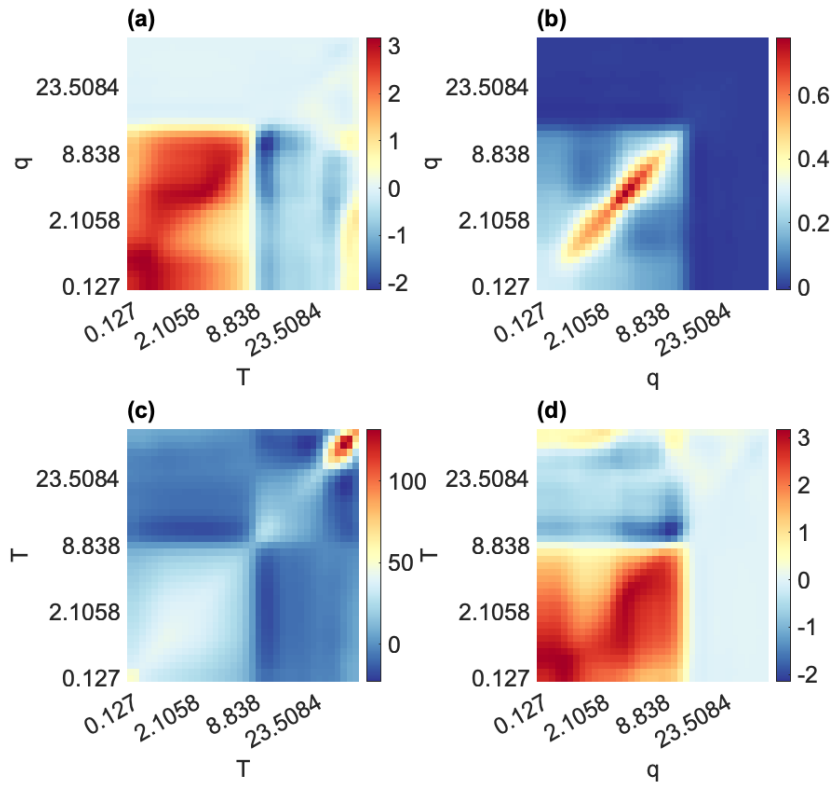


Figure S2. The vertical levels adopted in this study for all the retrievals. We utilize altitude coordinates for the retrievals, determined by averaging the geopotential heights from the a priori dataset.



**Figure S3. A priori covariance matrix  $S_\alpha$ .** Here, the label  $T$  represents temperature, and  $q$  represents the logarithm of the water vapor concentration. All units along the axes are in km.

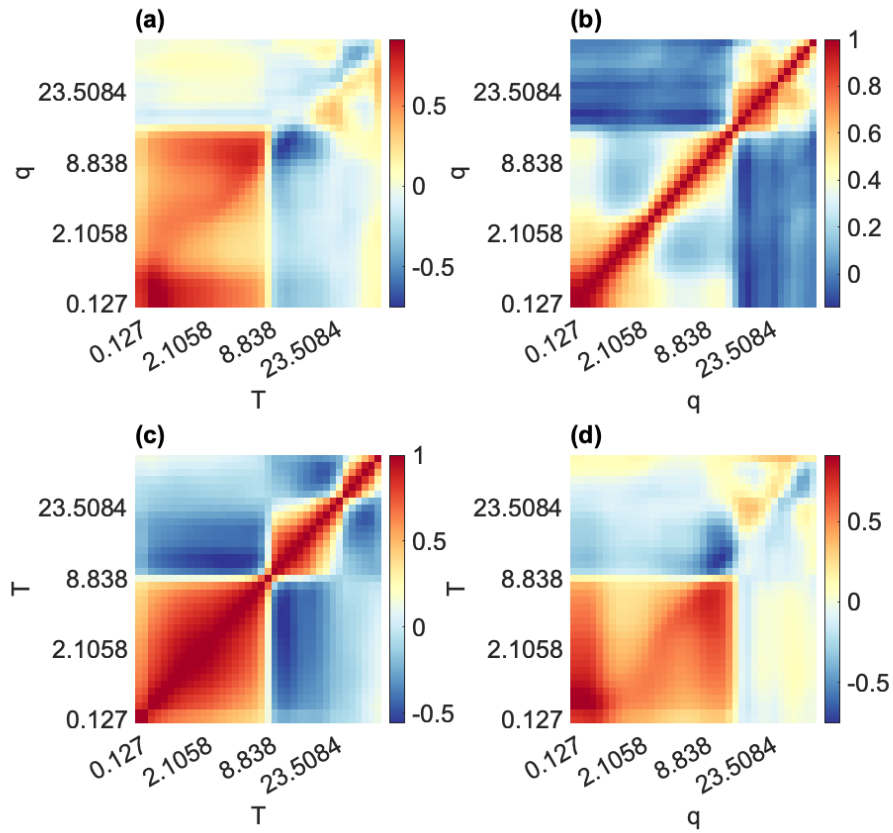
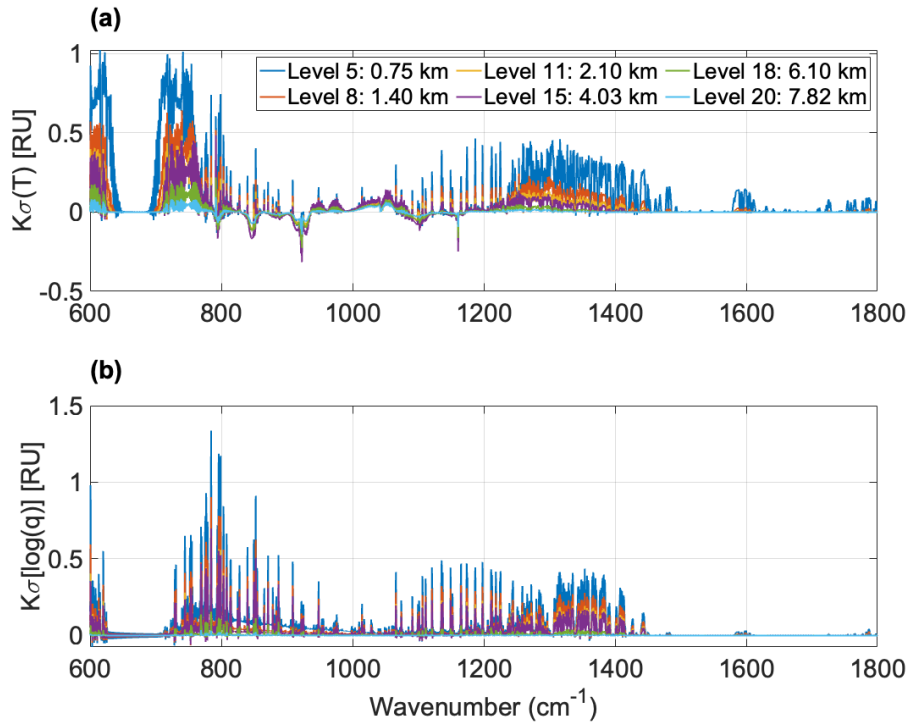


Figure S4. A priori correlation coefficient matrix  $C_a$ . Here, the label T represents temperature, and q represents the logarithm of the water vapor concentration. All units along the axes are in km.



**Figure S5.** (a)  $K_{AERI,T} \times \sigma(T)$  at selected levels. This shows the product of the temperature Jacobian,  $K_{AERI,T}$ , and the standard deviation of the temperature profiles in the a priori dataset,  $\sigma(T)$ . (b)  $K_{AERI,q} \times \sigma[\log(q)]$  at selected levels. This presents the product of the water vapor Jacobian,  $K_{AERI,q}$ , and the standard deviation of the water vapor concentration profiles in the a priori dataset,  $\sigma[\log(q)]$ . Note that we use the logarithm of water vapor concentration to calculate the water vapor Jacobian.

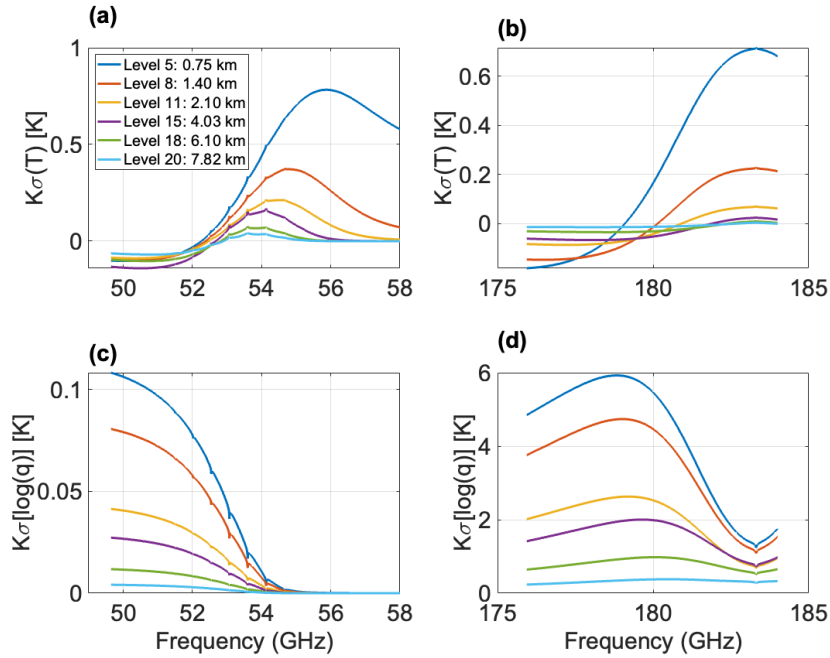


Figure S6. The same as Figure S5 but for HiSRAMS ground based zenith-pointing Jacobians. (a)  $K_{HISRAMS,T} \times \sigma(T)$  in the oxygen band. (b)  $K_{HISRAMS,T} \times \sigma(T)$  in the water vapor band. (c)  $K_{HISRAMS,q} \times \sigma[\log(q)]$  in the oxygen band. (d)  $K_{HISRAMS,q} \times \sigma[\log(q)]$  in the water vapor band.

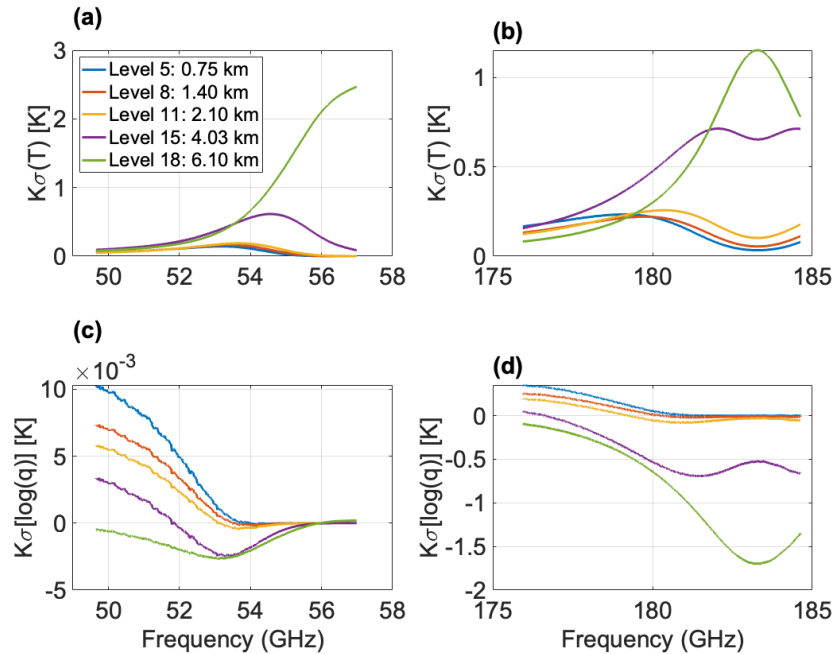
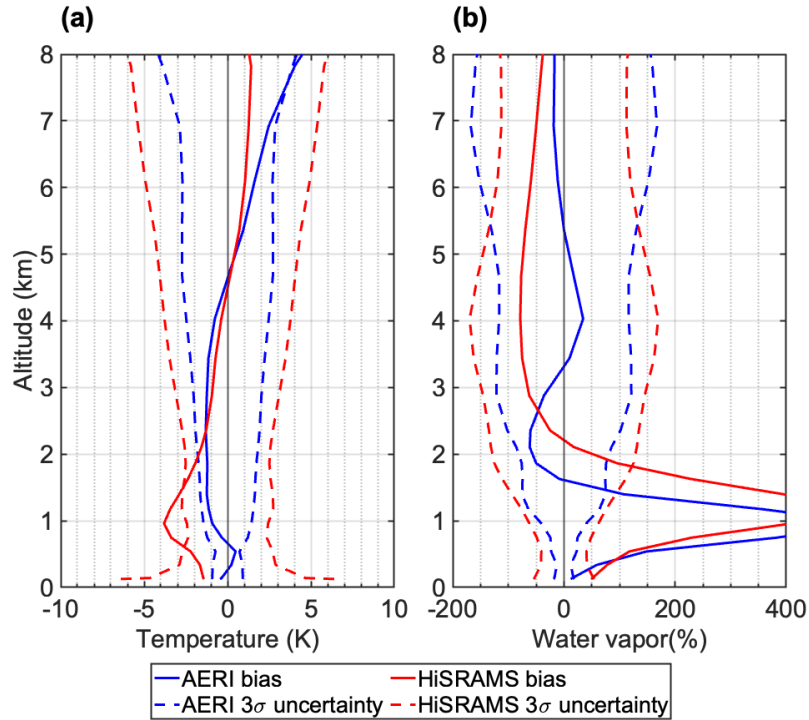


Figure S7. The same as Figure S6 but for HiSRAMS airborne nadir-pointing Jacobians. The observational height is set at 6.8 km.

## S2: Error analysis using smoothed truths

To reduce the relatively large retrieval bias around fine vertical features, we apply Eq. S1 to smooth the truth profiles obtained from radiosonde data. The error analysis results for both ground-based and joint retrievals are shown in Figures S8 and S9, respectively.

$$x_{truth}^{smoothed} = A(x_{truth} - x_a) + x_a \quad (S1)$$



**Figure S8: Comparison of retrieval bias and uncertainty in ground-based retrievals for (a) temperature and (b) water vapor. The truths used to determine the bias are smoothed using Eq. S1.**

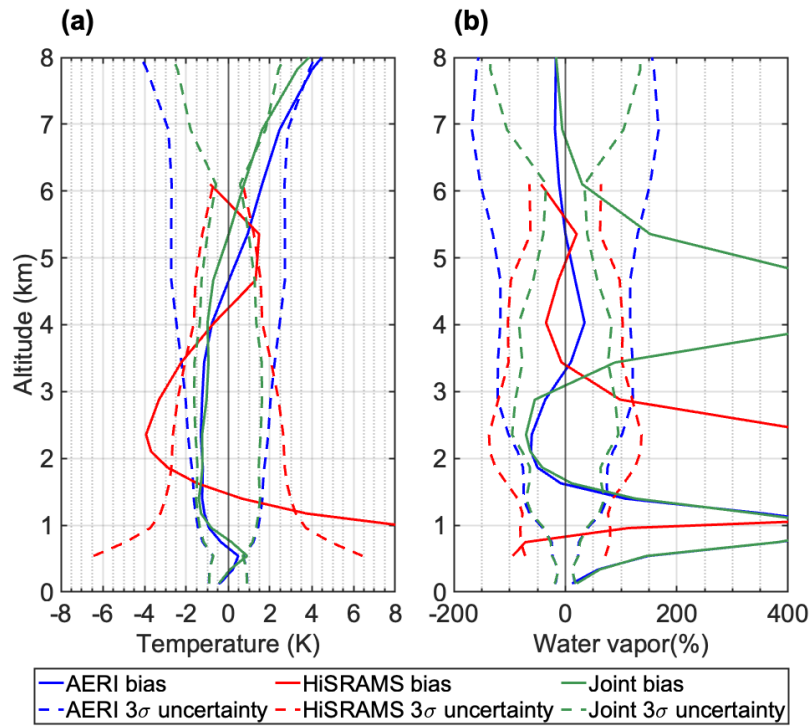


**Figure S9:** Comparison of retrieval bias and uncertainty in joint retrievals for (a) temperature and (b) water vapor. The truths used to determine the bias are smoothed using Eq. S1.



### S3: Comparison between observed and final simulated spectra

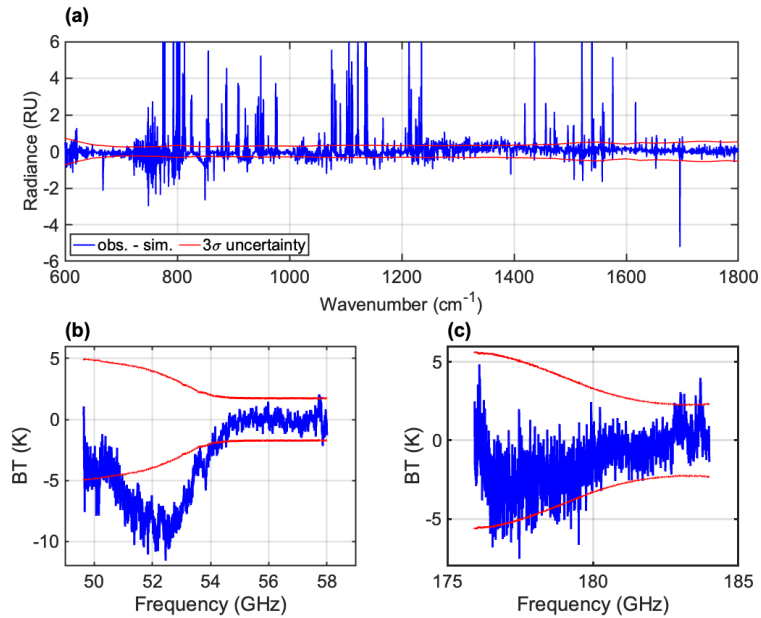


Figure S10: Radiance or brightness temperature differences between observations and the final retrieved simulation for ground-based retrievals: (a) AERI; (b) HiSRAMS oxygen band; (c) HiSRAMS water vapor band. The  $1\sigma$  uncertainties are determined from the square root of the diagonal components of  $S_e$ .

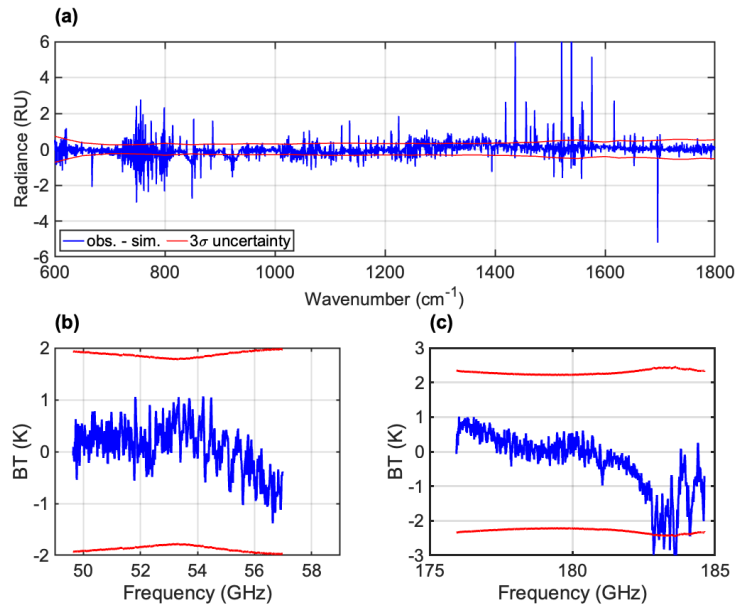


Figure S11: Radiance or brightness temperature differences between observations and the final retrieved simulation for joint retrievals: (a) AERI; (b) HiSRAMS oxygen band; (c) HiSRAMS water vapor band. The  $1\sigma$  uncertainties are determined from the square root of the diagonal components of  $S_e$ .